UAV Trajectories for Uniform Coverage in Convex Regions

Saeede Enayati
Electrical and Computer Engineering
University of Massachusetts, Amherst
senayati@umass.edu

Hossein Pishro-Nik
Electrical and Computer Engineering
University of Massachusetts, Amherst
pishro@umass.edu

2021 IEEE 93rd Vehicular Technology Conference (VTC2021-Spring) | 978-1-7281-8964-2/20/$31.00 ©2021 IEEE | DOI: 10.1109/VTC2021-Spring51267.2021.9448659

***Abstract*— In this paper, we introduce two general categories of stochastic trajectory processes that provide uniform Binomial distribution for unmanned aerial vehicles (UAVs) in finite convex areas with arbitrary geometry. First, we introduce radial trajectory process as a special case of the first category along with its properties. Then, we delve into the general trajectory processes, namely spiral and oval, and show that independent of the areas geometry, these trajectories not only provide uniform scattering of UAVs but also provide ergodic coverage across the area.**

***Index Terms*—Unmanned aerial vehicles, binomial point process, uniform network coverage, finite area.**

I. Introduction

Unmanned aerial vehicles (UAVs)-assisted communication networks are now a well-known network extension particularly in temporary and urgent use cases. Also, utilizing UAVs for data collection from the Internet of Things (IoT) devices and surveillance of urban, rural, and even inaccessible areas are of the most conceivable use cases of the UAVs in 5G and beyond 5G [1].

So far, the major part of research directions in UAV networks have been contributing to optimal placement and network modeling in the static networks. In this regard, a lot of studies have been done considering random modeling of UAV networks using tools from stochastic geometry, e.g., [2]–[4]. However, while numerous research endeavors have alluded to the static UAV communication networks, recently the mobility capability of the UAVs encouraged researchers to analyze and design mobile UAV networks too. In this regard, two research directions have been considered: path planning and performance nalysis using stochastic modeling of the mobile UAV networks. Although there exists an exhaustive literature on path planning and trajectory design, reviewing its state of the art is out of scope of this paper and interested readers are referred to [5].

Speaking of modeling and performance analysis of networks with mobile UAVs, stochastic trajectory models has been exploited in [6]–[9]. In [6], random waypoint mobility (RWPM) and uniform mobility (UM) were used to respectively model the vertical and spatial movements of the interfering UAVs in a finite network. Also, a more comprehensive model was developed in [7] where coverage probability was analyzed under the similar mixed mobility model and two UAV-user associations. Handover mobility was investigated in [9] for the third generation partnership project (3GPP) proposed mobility model in both constant and variable speed policies. The same authors also considered other models such as random stop (RS), random walk (RW), and random waypoint (RWP) in [8] to characterize the point processes of each mobility model and analyze the network performance in terms of average received rate and session rate. In our previous work [10] we introduced two families of stochastic trajectory processes that provide uniform coverage at each time instant in a finite circular area.

This work was supported by NSF under grant CNS-1932326.

Although the work in [10] provided general forms of stochastic trajectories, there is a limiting assumption: the region needs to be a circular area. However, this assumption is not true in many real-world scenarios. Hence, in this paper, we aim to extend the idea to the more practical case: general shaped convex areas. We show that there can be defined stochastic trajectory processes in any finite and convex area such that the uniformity of the points at each time instant can be preserved. We further show that the proposed trajectory processes exhibit an ergodic behavior in the following sense: the portion of the time that any area is covered over a long period is proportional to the area of that region.

The rest of this paper is as follows: Section II provides the system model and assumptions. Section III, introduces a simple but insightful stochastic trajectory process for the general finite convex area while Section IV provides the general form of this type of stochastic trajectories, called spiral trajectories. Section V, introduces the second form of general stochastic trajectory process families, namely oval trajectory processes and, Section VI concludes the paper.

Note: Throughout this paper, random variables are shown by bold small and capital letters while non random variables are shown by non-bold small and capital letters.

II. System Model and Assumptions

Figure 1 shows a general finite convex area in which the stochastic trajectories are of interests. The convex area is represented by $\mathcal{A}(\theta, \rho(\theta))$ in which $\theta \in (0, 2\pi)$ and $0 \le \rho(\theta) \le \rho_{max}$ are in polar coordinates. Without loss of generality, we assume that the origin is somewhere inside the region $\mathcal{A}$. Furthermore, there are a finite number of N UAVs aimed to fly over the area at the fixed altitude of H. The idea of the fixed altitude is fairly a reasonable assumption specially in a vast area with quiet large number of UAVs [2]. It is assumed that each UAV i, $i = 1, 2, ..., N$, starts its flight at random time instant $\mathbf{T}_i$ chosen independently and uniformly from $(0, \tau)$ where τ is an arbitrary time duration value for launching the

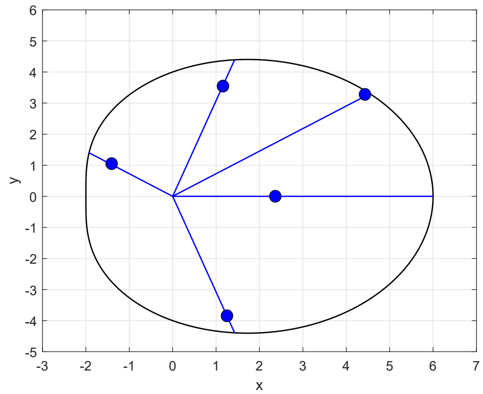

Fig. 1. A typical convex region. UAVs fly toward the regions boundaries and back on straight line trajectories which are selected by random angles, $\boldsymbol{\theta}_i$.

network. The more details on the UAVs mobility is provided specifically in each setup in the rest of the paper.

III. Radial Trajectory Process

In this part, we introduce the simplest form of trajectories, called radial trajectory in which UAVs move from the origin to the cell boundaries on a straight direction. As mentioned before, each UAV starts its flight at a random time instant chosen uniformly from $(0, \tau)$. Here, τ, is also the time it takes a UAV to reach the boundary of the area and vice versa. Prior to fly toward the cell boundaries, UAVs need to choose a random direction with respect to the horizontal axis. The angles $\boldsymbol{\theta}_i$s have to be selected such that the network experiences a uniform coverage across its region. This will be investigated in the next part. After reaching the edge of the area, UAVs are back to the origin in the same direction which takes τ seconds as well. Finally, when they get back to the origin, they choose another random direction and this procedure repeats continuously.

A. Uniformity

In this section, we show that for radial trajectory process a uniform BPP will be maintained at all times $t > \tau$ across any given convex area. Before going to the main part of this section, we first recall the distribution characterization of a uniform point process in a given area. The following lemma explicits the required characteristics of a uniformly scattered points in $\mathbb{R}^2$.

Lemma 1. *The joint probability function of the polar coordinates of uniformly distributed points in an arbitrary finite area $\mathcal{A}(\theta, \rho(\theta))$ in $\mathbb{R}^2$ is as below:*

$$f_{\mathbf{R},\boldsymbol{\Theta}}(r, \theta) = \frac{2r}{\int_0^{2\pi} \rho^2(\sigma) d\sigma}. \qquad (1)$$

Proof. We simply use the definition of the uniformity in $\mathbb{R}^2$ where $\mathbb{P}(\mathbf{X} \in dA) = \frac{dA}{|\mathcal{A}|}$, and $|.|$ is the Lebesgue measure. Hence, in an arbitrarily shaped area, with polar coordinates, $\mathcal{A}(\theta, \rho(\theta))$, this implies that

$$\mathbb{P}(\mathbf{X} \in dA) = \frac{r dr d\theta}{\int_0^{2\pi} \int_0^{\rho(\sigma)} r dr d\sigma} = f_{\mathbf{R},\boldsymbol{\Theta}}(r, \theta) dr d\theta, \qquad (2)$$

simplifying of which results in (1). □

Now based on this fact, we state Theorem 1 to introduce radial trajectory process in a general finite area. However, before the theorem, we first provide the necessary corresponding assumptions:

Assumption 1. *Assume that N UAVs choose their initial flight direction independently according to the probability distribution function (PDF) as below*

$$f_{\boldsymbol{\Theta}_i}(\theta_i) = \frac{\rho(\theta_i)^2}{\int_0^{2\pi} \rho(\sigma)^2 d\sigma}, \qquad i = 1, 2, ..., N. \qquad (3)$$

Also, conditioned on $\boldsymbol{\Theta}_\mathbf{i} = \theta_i$, the UAVs distance to the origin at each time instants of $k\tau + \mathbf{T}_i \leq t \leq (k+1)\tau + \mathbf{T}_i$ can be obtained as the following form

$$\mathbf{R}_{\mathbf{i}|\boldsymbol{\Theta}_\mathbf{i}=\theta_i}(t) = \begin{cases} \rho(\theta_i)\sqrt{\frac{t-\mathbf{T}_i-k\tau}{\tau}}, & k \text{ even} \\ \rho(\theta_i)\sqrt{\frac{(k+1)\tau-t+\mathbf{T}_i}{\tau}}, & k \text{ odd} \end{cases}, \qquad (4)$$

where $\mathbf{T}_i \sim U(0, \tau)$ is chosen independently.

Now the following theorem holds:

Theorem 1. *For all $t > \tau$, the instantaneous locations of the UAVs following Assumption 1 is a uniform BPP in any convex and finite area, $\mathcal{A}(\theta, \rho(\theta))$.*

Proof. To prove the theorem, we need to prove both the independence and uniformity of the points at each time instant $t > \tau$. The proof for the independence is straightforward for both the direction and the initial flight times of the UAVs are chosen independently. Therefore, we conclude that their location remains independent at all time instants after that. For the uniformity, we need to show that the UAVs locations represent a uniform scattered point process at each time $t > \tau$. To this end, we consider the path with direction from the origin to the boundaries where k is even. The proof for the inverse direction, i.e., when k is odd, is quiet similar. To do so, we first obtain the PDF of the UAVs distance to the origin by first calculating its cumulative distribution function (CDF) as below (For the sake of notation simplicity, we drop i from the letters.)

$$\begin{aligned} F_{\mathbf{R}|\boldsymbol{\Theta}}(r) &= \mathbb{P}\left[\rho(\theta)\sqrt{\frac{t-\mathbf{T}-k\tau}{\tau}} \leq r\right] \\ &= \mathbb{P}\left[\mathbf{T} \geq t - k\tau - \frac{\tau r^2}{\rho(\theta)^2}\right] \\ &= 1 - \frac{t}{\tau} + k + \frac{r^2}{\rho(\theta)^2}, \end{aligned}$$

derivative of which gives the conditional PDF, $f_{\mathbf{R}|\mathbf{\Theta}}(r|\theta)$ obtained as below

$$f_{\mathbf{R}|\mathbf{\Theta}}(r|\theta) = \frac{2r}{\rho(\theta)^2}. \quad (5)$$

This is equal to what one can obtain by dividing of (1) by Equation (3). On the other side, (3) can be verified by integrating from (1) with respect to the r. This completes the proof. □

Corollary 1. *Although choosing $\boldsymbol{\theta}_i$ using (3) is obtained mathematically, the intuition behind it is also interesting. Indeed, it shows that in order to be uniformly distributed, $\boldsymbol{\theta}_i$'s should be chosen such that those with larger distance to the origin are more probable. In other words, the longer the $\rho(\boldsymbol{\theta}_i)$ is, the more it is probable that $\boldsymbol{\theta}_i$ is chosen.*

Corollary 2. *The special case of Theorem 1 is when the area is simply a circle, i.e., $\rho(\theta) = \rho$. This case has already been investigated in [10].*

Corollary 3. *The time variant velocity of the i^{th} UAV can be obtained by taking derivation of (4) as below:*

$$\mathbf{V}_{\mathbf{i}|\mathbf{\Theta_i}=\theta_i}(t) = \begin{cases} \frac{\rho(\theta_i)}{\sqrt{\tau(t-\mathbf{T}_i-k\tau)}}, & k \text{ even} \\ -\frac{\rho(\theta_i)}{\sqrt{\tau((k+1)\tau-t+\mathbf{T}_i)}}, & k \text{ odd} \end{cases}, \quad (6)$$

where the negative sign shows the direction toward the origin.

In the next part, we investigate the ergodicity of the proposed process.

B. Coverage Ergodicity

In this section, we show that beside providing uniform distribution, radial trajectories provide ergodic coverage as well in the sense that the occupying time duration of any arbitrary region by the UAVs is proportional to its area. To show this, we assume a portion of region, $\mathcal{S} \subset \mathcal{A}$, and partition it to roughly equal small components of $\Delta s = \rho(\theta)\Delta\theta\Delta r \to 0$ and denote the random variable of the time duration that Δs_j is occupied in time interval of $(k\tau < t < (k+1)\tau)$ by $\mathbf{U}_{k,j}$. Now, we obtain the PDF of $\mathbf{U}_{k,j}$ in the following lemma.

Lemma 2. *The random variable U_k, j is distributed according to $U_k, j \sim \alpha\frac{\Delta r}{\rho(\theta_j)} Bernoulli(\delta_j)$ as shown below:*

$$\mathbf{U}_{k,j} = \begin{cases} \alpha\frac{\Delta r}{\rho(\theta_j)} & \text{with prob. } \delta_j \\ 0 & \text{with prob. } 1-\delta_j \end{cases}, \quad (7)$$

where $\alpha > 0$ is a constant and δ_j is the probability that a UAV has covered Δs_j which is obtained as in (9).

Proof. Let $\Delta s_j = \rho(\theta_j)\Delta r\Delta\theta$ be the area of each small component of $\mathcal{S}$. In the radial trajectory process, the probability that a region with area Δs_j is covered is equivalent to the probability of selecting the angle θ_j among the all possible angles which is obtained as

$$\mathbb{P}(\Delta s_j \text{ is covered}) = \delta_j = \frac{\int_{\theta_j}^{\theta_j+\Delta\theta}\rho(\sigma)^2 d\sigma}{\int_0^{2\pi}\rho(\sigma)^2 d\sigma}. \quad (8)$$

However, considering $\Delta\theta \to 0$ for all the components, we approximate (8) by

$$\delta_j = \frac{\Delta\theta\rho(\theta_j)^2}{\int_0^{2\pi}\rho(\sigma)^2 d\sigma} = \beta\Delta\theta\rho(\theta_j)^2, \forall j = 1, 2, \ldots, n, \quad (9)$$

where $\beta = \frac{1}{\int_0^{2\pi}\rho(\sigma)^2 d\sigma}$ and $n \to \infty$. Furthermore, the time duration in which an area of the size Δs_j is under coverage is conversely related to the UAVs velocity which is directly related to the distance from the center, i.e., $\rho(\theta_j)$. This is directly resulted from Equation (6). Hence, we may conclude that

$$\mathbf{U}_{k,j} = \alpha\frac{\Delta r}{\rho(\theta_j)}. \quad (10)$$

□

Now, using Lemma 2, we can obtain the expected coverage time of the area $\mathcal{S} = \lim_{n\to\infty}\bigcup_{j=1}^n \Delta s_j$ over the k^{th} period as below:

$$\mathbb{E}[\mathbf{U}_k] = \lim_{n\to\infty}\sum_{j=1}^n \mathbb{E}[\mathbf{U}_{k,j}] = \alpha\beta\lim_{n\to\infty}\sum_{j=1}^n \rho(\theta_j)\Delta r\Delta\theta, \quad (11)$$

where the last equation is obtained by multiplying Equations (9) and (10). Hence, we have

$$\mathbb{E}[\mathbf{U}_k] = \alpha\beta\lim_{n\to\infty}\sum_{j=1}^n \Delta s_j. \quad (12)$$

Finally, as $k \to \infty$, the total coverage time duration of $\mathcal{S}$ is obtained as below:

$$U_{\mathcal{S}} = \lim_{m\to\infty}\sum_{k=1}^m \mathbf{U}_k \overset{(a)}{=} \mathbb{E}[\mathbf{U}_k] = \alpha\beta\lim_{n\to\infty}\sum_{j=1}^n \Delta s_j = \alpha\beta|\mathcal{S}|, \quad (13)$$

where (a) comes from the Chernoff bound applied to the sum of i.i.d. Bernoulli random variables, $\mathbf{U}_k$, since according to which for random variable $\mathbf{Y} = \sum_{i=1}^n \mathbf{Y}_i$, where $\mathbf{Y}_i$s are i.i.d. Bernoulli random variables, we have

$$\mathbb{P}\left(|\mathbf{Y} - \mathbb{E}[\mathbf{Y}]| \geq \delta\mathbb{E}[\mathbf{Y}]\right) \leq 2e^{-\mu\zeta^2/3}, \quad \forall\ 0 < \zeta < 1.$$

Equation (13) represents the fact that as $k \to \infty$, the overall time duration in which $\mathcal{S} \subset \mathcal{A}$ is under coverage is directly proportional to its area.

In the next section, we extend the above idea to general trajectories.

IV. General Stochastic Trajectory Models: Spiral Trajectory Processes

In this section, we introduce a general form of radial trajectory, namely spiral trajectory process for convex, generally-shaped areas. Similar to the radial trajectory process, we show that the proposed general trajectory provides both a uniform and ergodic distribution.

A. Uniformity

In this section, we claim that for any convex arbitrarily-shaped region, we can define general trajectories that preserve uniformity of points at any time instant $t > \tau$. Theorem 2 states this idea. The basic idea is similar to what has been presented in [10]. In the following theorem, $\mathcal{A}(0, \rho(\theta))$ is the convex finite area with the origin in it. Before stating the theorem, first we provide a few assumptions and definitions:

Definition 1. *Let $X(s) = (x(s), y(s)) : s \in [0,1] \rightarrow \mathcal{A}(\theta, \rho(\theta))$, be the twice differentiable curves with the following properties:*

(a) $X(0) = 0, X(1) = \rho(\theta)$;
(b) $r(s) = |X(s)|$ is a strictly increasing function of s.

Assumption 2. *Assume that N UAVs start flying at times $\mathbf{T}_1, \mathbf{T}_2, \ldots, \mathbf{T}_N \sim U(0, \tau)$ to the direction with respect to the horizontal axis determined by $\mathbf{\Theta}_i \sim f_{\mathbf{\Theta}_i}(\theta_i)$, and using mappings of the form*

$$h(s) = \frac{\tau r(s)^2}{\rho(\theta_i)^2}, \tag{14}$$

they move toward the cell edge according to trajectories $X(s)$. Their mobility equation then becomes as (15) shown at the top of the next page, namely general spiral trajectories.

Theorem 2. *General spiral trajectories provide uniform BPP in finite convex areas for $t > \tau$.*

Proof. The proof is fairly similar to the proof of Theorem 1 in [10]. □

A typical $X(s)$ that satisfies Properties (1) and (2) can be determined as below

$$X(s) = (\rho(\theta) s^{k_1} \cos(\theta s^{k_2}), \rho(\theta) s^{k_1} \sin(\theta s^{k_2})), \tag{16}$$

where $k_1 > 0$, $k_2 \geq 0$. Figure 2 shows these trajectories in a region of the form $\rho(\theta) = a\cos(\theta) - b$.

Corollary 4. *The special case of radial trajectory can be obtained from spiral trajectories when $k_2 = 0$.*

B. Ergodicity

In this section, we show that the proposed spiral trajectories provide an ergodic coverage to the area. Similar to the radial trajectory, we define $\mathbf{U}_{k,j}$ as the time duration in which a very small area component, $\Delta s_j \in \mathcal{S}$ is under coverage at time interval $k\tau < t < (k+1)\tau$ and we aim to show that the time duration in which $\mathcal{S}$ is covered is proportional to its area. To this end, we first state the following lemma.

Lemma 3. *The coverage time duration of any small area component covered by spiral trajectories is a coefficient of a Bernoulli random variable as* (7).

Proof. Proof is similar to the proof of Lemma 2. Hence, the probability of Δs_j being covered is equal to (8). □

Now, we note that independent of the shape of trajectory, we can conclude that the time spent over any part of the region is proportional to its area. This is obtained from the fact that the key element in providing uniformity and ergodicity is the time mapping determined by (14). Hence, any form of trajectory that satisfies Definition 1, will result in a uniform and ergodic coverage probability as long as it follows mapping (14), or equivalently (15). Note that the convexity of the region is a fundamental assumption in the above developed framework. Otherwise, one can easily provide counter examples for the obtained results.

V. General Stochastic Trajectory Models: Oval Trajectory Processes

In this section, we introduce the second family of general trajectory processes for convex regions and show its uniformity and ergodicity across the area. In this trajectory model, UAVs move across a series of closed paths around the origin of the area. The details are as follows.

Assumption 3. *Assume that N UAVs choose their flight times, $\mathbf{T}_1, \mathbf{T}_2, \ldots, \mathbf{T}_N$ uniformly from $(0, \tau)$. Also, assume that they choose path lengths $l_1, l_2, ..., l_N$ independently and uniformly with the following probability mass function:*

$$P_{\mathbf{L}_i}(l_i) = \frac{l_i}{L}, \qquad i = 1, 2, \ldots N, \tag{17}$$

where $L = \sum_{i=1}^{N} l_i$ [1]*. In addition, note that the paths need to be closed and continuously differentiable. The UAVs can start their flight from any point of their path. Furthermore, assume that it takes τ seconds for each UAV to complete a round of its flight. We call this trajectory model oval trajectory process.*

Theorem 3. *The oval trajectories provide uniform BPP in any convex area.*

Proof. The proof of independence is straightforward, since each UAV independently chooses its flight start time and path. The idea to show that the distribution of the UAVs locations is uniform is to consider two area components and show that the probability of choosing these two components is the same. As shown in Figure 3, consider two paths l_k and l_j. Also, consider small area components of these two paths ΔA_k and ΔA_j where $\Delta A_k = \Delta A_j$. The probability of choosing ΔA_k is written as

$$P_{\Delta A}(\Delta A_k) = \frac{l_k}{L} \times \frac{\Delta A_k}{C l_k}, \tag{18}$$

where $C > 0$ is a constant. Similarly, the probability of choosing ΔA_j is written as

$$P_{\Delta A}(\Delta A_j) = \frac{l_j}{L} \times \frac{\Delta A_j}{C l_j}. \tag{19}$$

Therefore, $P_{\Delta A}(\Delta A_k) = P_{\Delta A}(\Delta A_j)$ which means that any point in the region can be occupied by a UAV with the same probability as the others. Hence, the UAVs are distributed uniformly. □

[1] To avoid collision, we assume that at each setup, paths are designed by the same shape while having different lengths. In this framework, $\cup_{i=1}^{\infty} l_i = \mathcal{A}(\rho, \Theta)$ and $\cap_{i=1}^{\infty} l_i = \emptyset$.

$$(\tilde{\mathbf{x}}_i(t), \tilde{\mathbf{y}}_i(t)) = \begin{cases} \left(x_i(h_i^{-1}(t - k\tau - \mathbf{T}_i)), y_i(h_i^{-1}(t - k\tau - \mathbf{T}_i)) \right), & k \text{ even} \\ \left(x_i(h_i^{-1}((k+1)\tau + \mathbf{T}_i - t)), y_i(h_i^{-1}((k+1)\tau + \mathbf{T}_i - t)) \right), & k \text{ odd} \end{cases}. \quad (15)$$

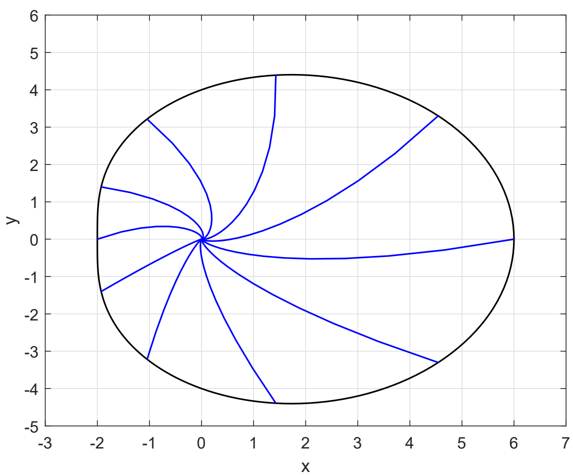

Fig. 2. General curves obtained from Equation (16) where $k_1 = 25$ and $k_2 = 2$, in $\mathcal{A}(\theta, \rho(\theta)) = 2 - 4\cos(\theta)$.

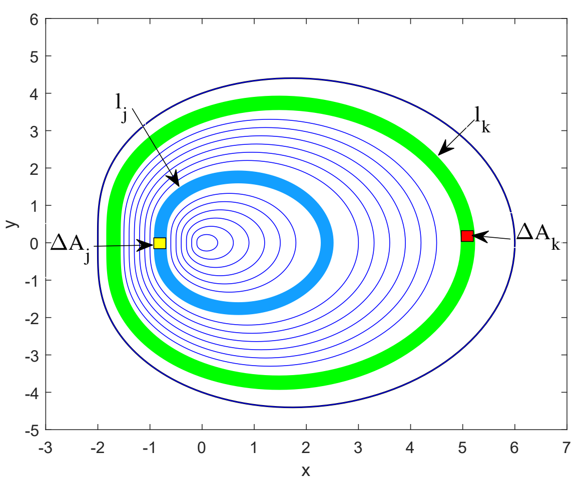

Fig. 3. Oval trajectories. Note that for the proof, we assume that trajectories have a small width (e.g., the green and the blue curves) which asymptotically goes to zero.

A. Ergodicity

Similar to the previous processes, oval trajectories provide ergodic coverage in the sense that the coverage time duration of any part of the region is proportional to its area over a long period. To show this, we consider $\mathcal{S} \subset \mathcal{A}$ and provide the following lemma.

Lemma 4. *The coverage time duration of a small area component $\Delta A_j \to 0$ under oval trajectory process is a coefficient of a Bernoulli random variable as below*

$$\mathbf{W}_{k,j} = \begin{cases} \frac{\Delta A_j}{C l_j}\tau & \textit{with prob.} \quad \delta_j \\ 0 & \textit{with prob.} \quad 1 - \delta_j \end{cases}, \quad (20)$$

where $\delta_j = \frac{l_j}{L}$.

Proof. The proof is similar to the proof of Lemma 2. □

Therefore, The overall coverage time duration over $\mathcal{S}$ is obtained as

$$W = \lim_{m\to\infty} \sum_{k=1}^{m} \mathbf{W}_k \overset{(a)}{=} \mathbb{E}[\mathbf{W}_k] = \frac{\tau}{CL} \lim_{n\to\infty} \sum_{j=1}^{n} \Delta A_j$$
$$= \frac{\tau}{CL}|\mathcal{S}|, \quad (21)$$

where (a) results from Chernoff bound.

VI. Conclusion

In this paper, general stochastic trajectory processes were introduced for arbitrarily-shaped convex areas such that uniform point distribution for a finite number of UAVs is obtained. We investigated two general categories namely spiral and oval, and showed that at each time instant, the trajectories can provide both uniform and ergodic distribution across the area.

References

[1] B. Li, Z. Fei, and Y. Zhang, "UAV communications for 5G and beyond: Recent advances and future trends," *IEEE Internet of Things Journal*, vol. 6, no. 2, pp. 2241–2263, April 2019.

[2] V. V. Chetlur and H. S. Dhillon, "Downlink coverage analysis for a finite 3D wireless network of unmanned aerial vehicles," *IEEE Transactions on Communications*, vol. 65, no. 10, pp. 4543–4558, Oct. 2017.

[3] E. Turgut and M. C. Gursoy, "Downlink analysis in unmanned aerial vehicle (uav) assisted cellular networks with clustered users," *IEEE Access*, vol. 6, pp. 36 313–36 324, May 2018.

[4] Y. Zhu, G. Zhang, and M. Fitch, "Secrecy rate analysis of UAV-enabled mmwave networks using matern hardcore point processes," *IEEE Journal on Selected Areas in Communications*, vol. 36, no. 7, pp. 1397–1409, July 2018.

[5] M. Mozaffari, W. Saad, M. Bennis, Y.-H. Nam, and M. Debbah, "A tutorial on UAVs for wireless networks: Applications, challenges, and open problems," *IEEE communications surveys & tutorials*, vol. 21, no. 3, pp. 2334–2360, Thirdquarter 2019.

[6] P. K. Sharma and D. I. Kim, "Coverage probability of 3D mobile UAV networks," *IEEE Wireless Communications Letters*, vol. 8, no. 1, pp. 97–100, Feb. 2019.

[7] ——, "Random 3D mobile UAV networks: Mobility modeling and coverage probability," *IEEE Transactions on Wireless Communications*, vol. 18, no. 5, pp. 2527–2538, May 2019.

[8] M. Banagar and H. S. Dhillon, "Performance characterization of canonical mobility models in drone cellular networks," *IEEE Transactions on Wireless Communications*, vol. 19, no. 7, pp. 4994–5009, July 2020.

[9] M. Banagar, V. V. Chetlur, and H. S. Dhillon, "Handover probability in drone cellular networks," *IEEE Wireless Communications Letters*, vol. 9, no. 7, pp. 933–937, July 2020.

[10] S. Enayati, H. Saeedi, H. Pishro-Nik, and H. Yanikomeroglu, "Moving aerial base station networks: stochastic geometry analysis and design perspective," *IEEE Transactions on Wireless Communications*, vol. 18, no. 6, pp. 2977 – 2988, June 2019.